

贵州紫云泥盆系重晶石矿床中与古甲烷渗漏事件有关的球状灰岩成因厘定

张旭¹⁾, 高军波¹⁾, 杨瑞东¹⁾, 陈军¹⁾, 郑禄林¹⁾, 魏怀瑞¹⁾, 鲍森²⁾

1) 贵州大学资源与环境工程学院, 贵阳, 550025;

2) 贵州省地质矿产勘查开发局 112 地质大队, 贵州安顺, 561000

内容提要: 关于古代冷泉碳酸盐岩的报道主要集中于新元古代“盖帽”碳酸盐岩和晚古生代以来(特别是石炭纪以来)的沉积地层中,与沉积矿床伴生的冷泉碳酸盐岩的研究鲜有报道。本文通过对贵州紫云泥盆系大型重晶石矿床中新发现的球状、椭球状灰岩进行详细地野外观察,并结合矿物学、元素地球化学和 C—O 同位素研究,探讨并揭示了灰岩的成因和形成环境,以及与古甲烷渗漏事件之间的关系。结果表明:灰岩呈球状、椭球状、管状顺层产于重晶石之中及其下部地层。灰岩中发育大量类似现代海底冷泉沉积碳酸盐岩的凝块和草莓状黄铁矿;草莓状黄铁矿内部结构呈葵花状,组成葵花状的单颗黄铁矿大小基本一致,轮廓清晰。灰岩较低的 $\delta^{13}\text{C}_{\text{V-PDB}}$ 值(- 10.3‰)表明其碳源主要为热解成因甲烷气或混合气。灰岩 Ce/Ce* 值除反映古沉积环境为还原状态外,也指示间歇性氧化状态的存在,这可能与甲烷气体的渗漏速率有关。

关键词: 灰岩; 沉积结构; 碳氧同位素; 稀土元素; 泥盆系; 紫云

冷泉与冷泉碳酸盐岩是近年来地质学研究的热点,国内外学者普遍关注。冷泉碳酸盐岩是海底甲烷渗漏作用形成的典型矿物之一,是研究海洋沉积环境变化(Tryon et al., 2004; Lu Yang et al., 2014)、厘定重大地质事件的重要指示器(Wu Shiguo et al., 2002),其明显偏负的 $\delta^{13}\text{C}_{\text{V-PDB}}$ 值是区别是否为冷泉成因碳酸盐岩的最关键标志(Peckmann et al., 1999a, 2001; Kennedy et al., 2001; Jiang Ganqing et al., 2003)。近年来,已在世界各地的大陆边缘及其附近区域发现大量现代海底冷泉成因碳酸盐岩。例如:墨西哥湾(Canet et al., 2006; Birgel et al., 2011; Feng Dong et al., 2011)、加利福尼亚湾(Canet et al., 2010)、尼日尔三角洲(Bayon et al., 2011)、中国南海(陈多福等, 2005; 陈忠等, 2006; 陆红锋等, 2006; Chen Duofu et al., 2005; Ge Lu et al., 2010; Wang Shuhong et al., 2014)和日本海(Watanabe et al., 2008)等,科学家对这些冷泉碳酸盐岩已开展了系统地研究,取得了大量研究成果。

关于古代冷泉成因碳酸盐岩的报道有很多,主要集中于晚古生代以来的沉积地层(Campbell et al., 2002; Peckmann et al., 1999b, 2001, 2004; Jenkins et al., 2007; Himmler et al., 2008; Conti et al., 2010; Hammer et al., 2011)。此外,新元古代陡山沱期的盖帽碳酸盐岩也被认为属于冷泉成因(Kennedy et al., 2001, 2008; Jiang Ganqing et al., 2003; Wang Jiasheng et al., 2008),但有学者对此提出质疑(Hoffman et al., 1998)。我国古代冷泉碳酸盐岩的发现与研究也取得进展,Tong Hongpeng 等(2012)首先报道了西藏日喀则产于白垩系地层中的冷泉碳酸盐岩,这些冷泉碳酸盐岩以粒径介于 3 ~ 20 cm 不等的球状、椭球状顺层产出,碳酸盐岩与围岩界限清楚,且普遍具有偏负的 $\delta^{13}\text{C}_{\text{V-PDB}}$ 值(介于 - 27.7‰ ~ - 4.0‰)。欧莉华等(2013)报道了内蒙古西乌珠穆沁旗林哈日根台苏木二叠系林西组地层中的结核状碳酸盐岩碳氧同位素研究结果,认为属于冷泉成因。李艳菊等(2013)和夏国清等

注: 本文为国家自然科学基金资助项目(编号:41503030)、贵州省科技合作计划项目(编号:黔科合 LH 字[2015]7663 号)和贵州大学人才引进项目(编号:贵大人基合字 201454 号)的成果。

收稿日期:2016-05-13; 改回日期:2017-04-06; 责任编辑:章雨旭。Doi: 10.16509/j.georeview.2017.03.007

作者简介: 张旭,男,1991年生,硕士研究生。研究方向为沉积矿床。Email: zhangxu199108@163.com。通讯作者: 高军波,男,1985年生。博士,副教授。主要从事沉积矿床教学及科研工作。Email: gaojunbo1985@126.com。

(2015)也相继在羌塘盆地双湖地区发现冷泉活动的证据,这些发现为研究古代冷泉碳酸盐岩提供了重要的研究实例和参考。

通过对已有成果的梳理和分析,冷泉碳酸盐岩在古代沉积型矿床中的分布相对较少,已报道的研究实例很有限。周琦等(2007)通过对贵州铜仁大

塘坡期含锰岩系和下伏地层白云岩碳氧同位素进行研究,认为它们均是甲烷渗漏作用的产物,并提出甲烷渗漏作对锰矿形成有重要控制。Canet 等(2014)对墨西哥湾西北部 Sonora 层状重晶石矿床中碳酸盐岩的 C—O 同位素组成进行研究,并结合重晶石 S 和 Sr 同位素数据,提出产于层状重晶石矿中的碳酸

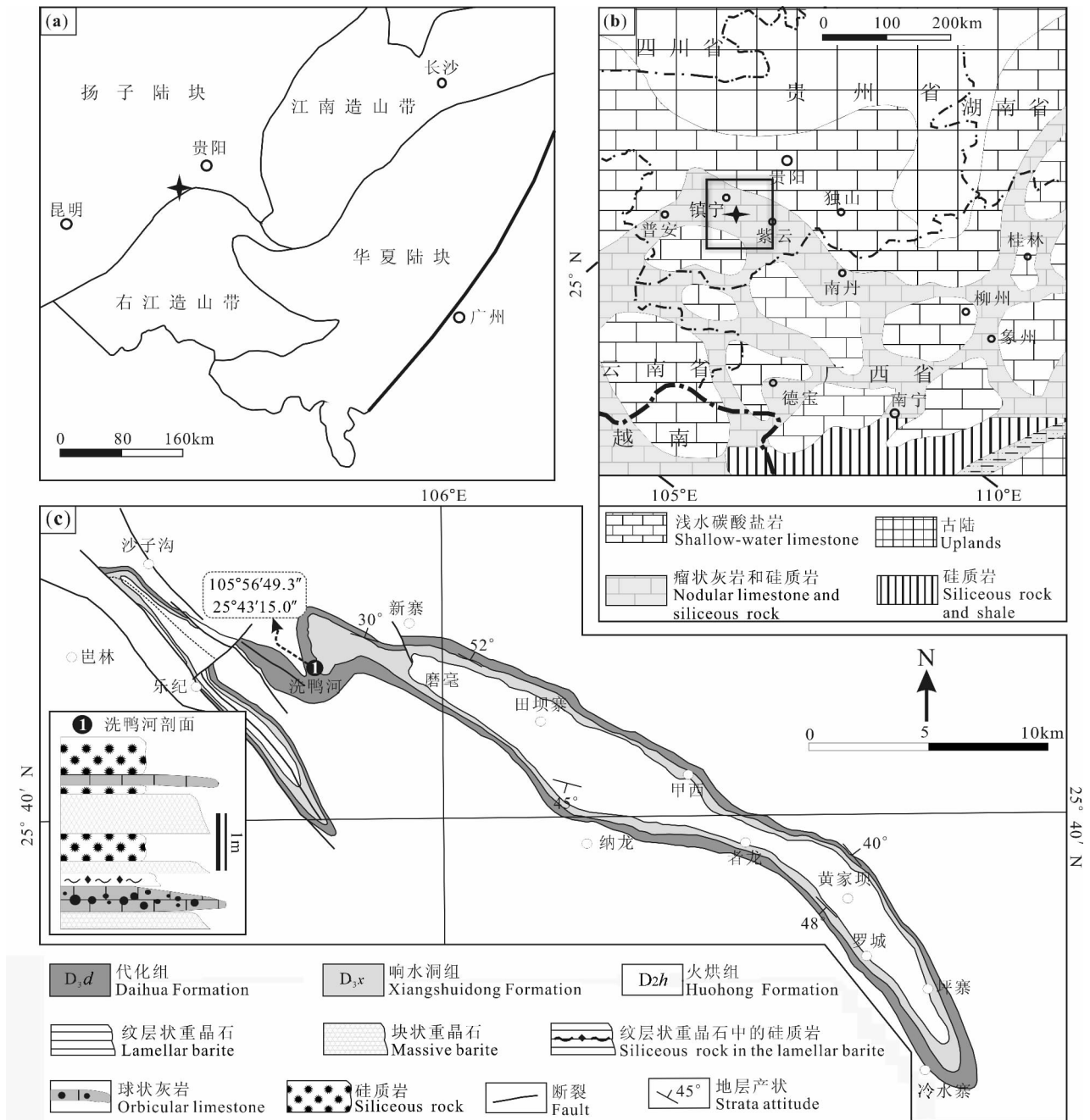


图 1 贵州紫云洗鸭河重晶石矿床区域地质背景与矿区地质图: (a) 区域地质简图 (据程裕淇, 1994);

(b) 研究区晚泥盆世古地理图 (据 Chen Daizhao et al., 2001); (c) 矿区地质与地层沉积柱状图

Fig. 1 Geological setting and geological map of Xiyaher barite deposit, Ziyun, Guizhou: (a) Regional geological map of Xiyaher barite deposit in Ziyun (after Cheng Yuqi, 1994#); (b) paleogeographic reconstruction of the research area during the Late Devonian (after Chen Daizhao et al., 2001); (c) sediment column, geological map of the Xiyaher barite deposit

盐岩为冷泉成因。紫云泥盆系重晶石矿床是中国泥盆系沉积型重晶石矿床的典型代表,通过系统地野外观察,在紫云泥盆系重晶石矿区洗鸭河矿段发现大量球状、椭球状和管状灰岩,它们顺层产于重晶石矿层之下或其中,灰岩与围岩界限清晰。基于球状、椭球状和管状灰岩产出特征,并结合已获得的有关镇宁—紫云泥盆系重晶石矿床研究成果,认为这些灰岩可能与甲烷渗漏作用有一定关联。

为此,本文在前人研究工作基础上,对紫云洗鸭河重晶石矿床中球状、椭球状和管状灰岩进行了详细矿物学、元素地球化学和 C—O 同位素组成研究,认为灰岩是深水裂陷盆地边缘发生的甲烷渗漏作用的产物。这一认识对于深入理解镇宁—紫云泥盆系重晶石矿床成因与成矿机理有重要指示意义,对于了解华南泥盆纪古海洋环境状况也是一种很好的借鉴。

1 地质背景和样品特征

1.1 地质背景

紫云洗鸭河位于右江造山带与扬子陆块过渡部位(图 1a)。晚古生代,由于区内北西向区域性断裂强烈活动(以裂解为主),控制着包括研究区在内的整个右江盆地的古地貌演化,并形成了多个规模不等的深水裂陷盆地(杜远生等, 2013)。其中,呈北西—南东向自贵州赫章延伸至广西南丹的水城—紫云—南丹深大断裂活动形成的深水裂陷槽盆是贵州西部重要的构造单元之一,对区内构造演化、古地理—环境变化及成矿作用均有明显控制(高军波等, 2015)。该深水槽盆呈北西窄、南东宽的楔形,地表延伸大于 400 km,宽度介于 10~80 km(王尚彦等, 2006),内部产出有镇宁—紫云泥盆系大型重晶石矿床、赫章—威宁泥盆系菱铁矿、广西南丹大厂锡多金属等(高军波等, 2015)。本文研究的球状、管状灰岩就产于镇宁—紫云泥盆系大型重晶石矿之中。

水城—紫云—南丹深大断裂是一条切割深、延伸远、活动周期长的区域性断裂,对整个贵州西部自晚古生代以来的构造演化和区域成矿作用有深远影响,充当着右江盆地北缘的边界断裂,是贵州省省级构造单元划分的重要依据之一。毛健全等(1997)研究认为该断裂局部切入上地幔,是连通地表和深部物质和流体循环、对流的重要通道。早中泥盆世,随着华南古特提斯洋逐渐打开(Hara et al., 2010),右江盆地进入伸展、断裂阶段,并形成独具特色的深

水台沟与浅水碳酸盐岩台地相间排列的古地理格局(图 1b)。同时,这一区域性地质事件间接导致水城—紫云—南丹深大断裂及其控制的裂陷盆地不断发生水平拉张并沿北西方向形成裂陷深水槽盆。中晚泥盆世,水城—紫云—南丹深大断裂控制的深水槽盆中主要沉积硅质岩、炭质泥岩、灰岩,镇宁—紫云泥盆系大型重晶石就产于深水槽盆中沉积的硅质岩中。重晶石矿体主要呈北西—南东向展布于镇宁乐纪至紫云罗城,水平延伸长度约 40 km。产于重晶石矿中的球状、椭球状和管状灰岩主要见于紫云洗鸭河矿段和罗城矿段,其中洗鸭河矿段灰岩分布最多,结构构造类型最全(图 1c)。

1.2 样品特征

详细地野外调查发现,紫云洗鸭河矿段发育类似甲烷渗漏的通道或喷口构造(图 2a、b),喷口直径约 5~10cm,局部可见同心圆构造。古喷口中心见浅灰色灰泥。这些古甲烷渗漏通道和喷口构造位于层状重晶石底部,构成通道或喷口的岩石类型以深灰色细晶灰岩为主,其边部见纹层状硅质灰岩包裹。本文重点研究的球状和管状灰岩样品主要采自于洗鸭河剖面,灰岩呈球状、椭球状、管状展布于重晶石层之下,一些球状灰岩产于重晶石层之中(图 2c)。球状灰岩粒径介于 5~70 cm,管状灰岩长度最长达 60 cm,与围岩接触关系清楚,围岩(黑色、灰黑色炭质泥岩)层理常绕过球状、椭球状和管状灰岩,指示了同沉积形成特征(图 2c、d)。

洗鸭河重晶石矿床中球状、椭球状灰岩呈灰色、深灰色致密块状,部分因遭受后期氧化,表面呈土黄色。已有研究揭示,冷泉渗漏区常发生多种生物、化学作用,硫酸盐还原细菌作用下发生的甲烷缺氧氧化,往往可以形成自生碳酸盐岩和单硫化物(Boetius, 2000)。当碳酸盐岩局部饱和则发生碳酸盐岩矿物沉淀,形成凝块状微晶灰岩、放射状和葡萄状文石胶结物(Stakes et al., 1999)。通过高精度扫描电镜观察研究,发现洗鸭河剖面球状、椭球状灰岩显微组构主要由微—细晶碳酸盐岩矿物组成,且发育较多碳酸盐岩凝块,凝块粒径介于 30~100 μm (图 2e)。另外,灰岩中可见大量微细粒草莓状黄铁矿,黄铁矿粒径介于 1~4 μm 之间(图 2f、g)。扫描电镜观察发现,草莓状黄铁矿微观结构相对简单,呈葵花状。葵花状黄铁矿中黄铁矿单晶颗粒形态保存完整,轮廓清晰,多呈不规则四边形、五边形、六边形密集簇团分布。部分靠近葵花状黄铁矿集体体边缘的黄铁矿遭受溶蚀使得边界较为模糊(图 2h)。

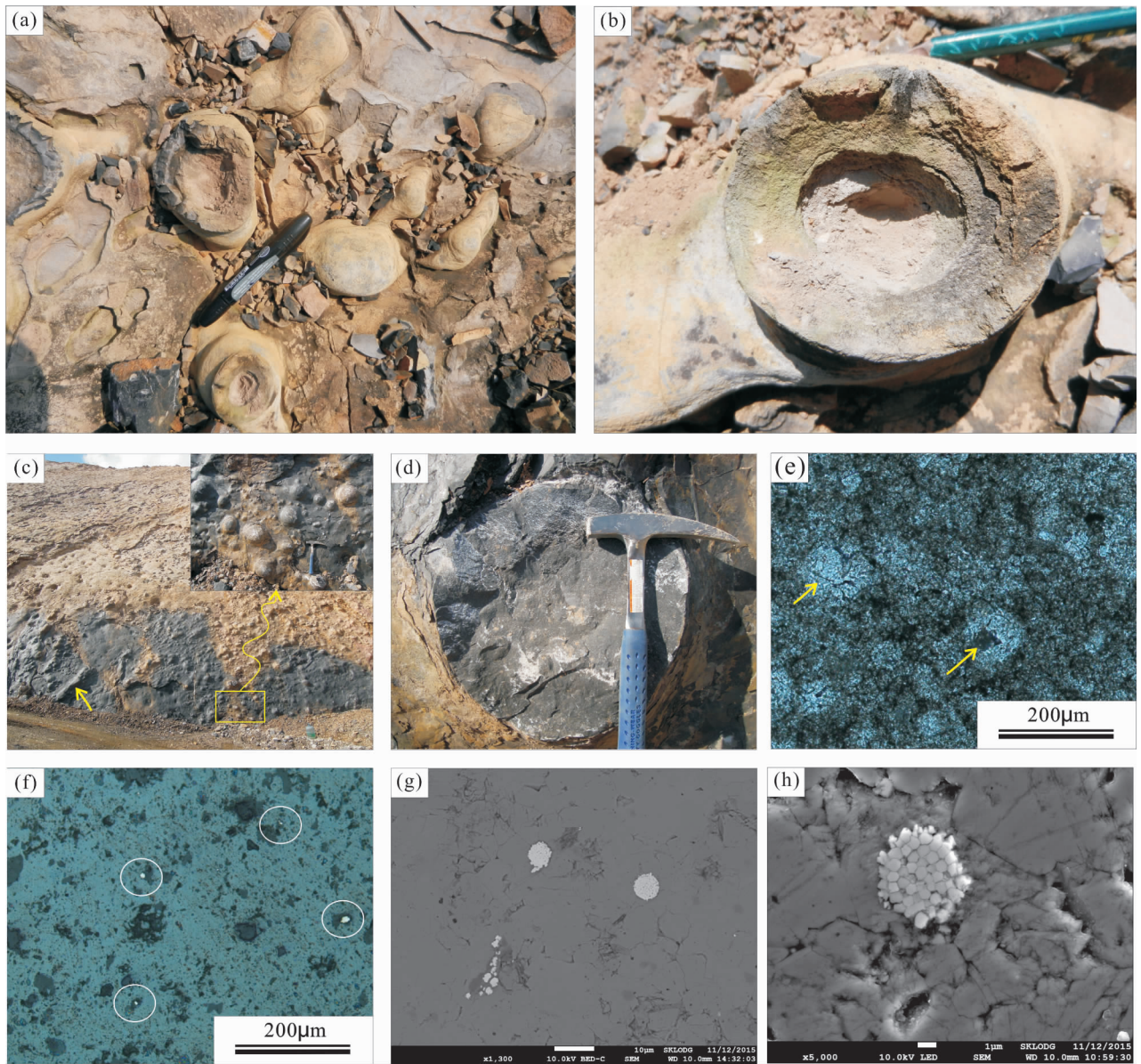


图 2 贵州紫云洗鸭河球状灰岩野外产状与显微结构特征

Fig. 2 Photographs of the geological features and microstructure of the spherical limestone of Xiyaherite deposit, Ziyun, Guizhou

(a) 和 (b) 类似甲烷渗漏的通道和喷口特征; (c) 球状、管状 (黄色箭头所指) 灰岩野外产出特征; (d) 围岩层理绕过球状灰岩, 两者接触界限清楚; (e) 灰岩中的碳酸盐岩凝块 (黄色箭头所指) (正交偏光); (f) 球状灰岩中分布的微细粒黄铁矿 (白圈所示) (正交偏光); (g) 零星散布的草莓状黄铁矿; (h) 黄铁矿颗粒密集排列呈葵花状

(a) and (b) images of the methane seepage from Xiyaherite deposit in Ziyun; (c) spherical, tubular limestones (yellow arrow); (d) the bedding of surrounding rocks (siliceous mudstone) around the spherical limestone; (e) clotted micrites are observed in spherical limestone (yellow arrows) (cross polarized light); (f) fine-grained pyrite are observed in spherical limestones (white circle) (cross polarized light); (g) the framboidal pyrite, which is sporadic distributed; (h) the internal structure of framboidal pyrite is simple, which has the form of sun-flower

2 分析方法

通过对紫云泥盆系重晶石矿区洗鸭河矿段中球状、椭球状和管状灰岩野外地质特征的详细观察, 采集新鲜无污染的灰岩样品 9 件。样品显微结构观察

在中国科学院地球化学研究所矿床地球化学国家重点实验室进行, 实验仪器为高精度场发射扫描电镜。

主量元素测试在澳实矿物实验室 (广州) 完成。测试流程为: 将 200 目的灰岩样品进行硼酸锂 - 硝

酸锂熔融,熔融物冷却后加入稀 HNO_3 和稀 HCl 溶解,然后采用 X 荧光光谱分析法进行测试。

稀土元素测试在中国科学院地球化学研究所矿床地球化学国家重点实验室完成,选用仪器为加拿大 PerkinElmer 公司生产的 ELAN DRC-e 四级杆型电感耦合等离子体质谱(Q-ICP-MS)。分析步骤为:称取 200 目灰岩样品 50 mg 放置于封闭容样装置中,加入 1mL HF,放置电热板上蒸干,再加入 1mL HF 和 0.5mL HNO_3 再蒸干,上述过程重复一次,最后加入 2mL HNO_3 和 5mL 水,密封并放置于 130 °C 溶解残渣 3 h,取出冷却后加入 500ng Rh 内标溶液,转移至 50 mL 离心管中,最后在 Q-ICP-MS 上进行测试,分析精度优于 5%。详细测试方法见 Qi Liang 等(2000)。

碳氧同位素测试用磷酸法在中国科学院地球化学研究所环境地球化学国家重点实验室完成,选用 Thermo Finnigan 公司生产的 Gas Bench II 和 Delta Plus AD 同位素质谱仪相连接在线磷酸法分析。分析过程插入碳酸盐岩固体标准,以校正测定结果。所有测试结果均相对于 V-PDB 标准,分析绝对误差 $\delta^{13}\text{C}$ 优于 $\pm 0.05\text{‰}$, $\delta^{18}\text{O}$ 优于 $\pm 0.08\text{‰}$ 。

3 分析结果

3.1 主量元素

主量元素测试结果见表 1。9 件样品 CaO 含量为 45.1% ~ 55.1%、 SiO_2 含量为 2.21% ~ 17.75% ,

表 1 贵州紫云洗鸭河泥盆系重晶石矿中灰岩主量元素分析结果(%)

Table 1 Major element contents (%) of limestone in Devonian barite deposit in Xiyah, Ziyun County, Guizhou

样品号	XYH01	XYH02	XYH03	XYH04	XYH05	XYH06	XYH07	XYH08	XYH09
Al_2O_3	0.11	0.4	0.57	0.17	0.16	0.76	0.27	0.03	0.22
BaO	0.02	0.06	0.05	0.02	0.05	0.04	0.02	0.04	0.15
Cr_2O_3	<0.01	<0.01	<0.01	<0.01	<0.01	<0.01	<0.01	<0.01	<0.01
CaO	53.8	45.2	51.2	52.2	50.9	45.5	48.9	55.1	51.4
TFe_2O_3	0.05	0.19	0.18	0.09	0.07	0.24	0.12	0.04	0.1
K_2O	0.03	0.09	0.11	0.03	0.05	0.15	0.06	0.02	0.04
MgO	0.23	0.25	0.3	0.37	0.45	0.31	0.25	0.37	0.18
MnO	0.01	0.05	0.01	<0.01	0.09	0.01	0.08	0.03	0.16
P_2O_5	0.03	0.04	0.06	0.08	0.1	0.09	0.04	0.06	0.02
Na_2O	<0.01	0.01	<0.01	<0.01	<0.01	<0.01	<0.01	<0.01	<0.01
SO_3	0.11	0.21	0.12	0.14	0.12	0.09	0.2	0.07	0.16
SiO_2	4.79	17.75	7.84	5.76	7.94	16.92	12.36	2.22	8.14
TiO_2	0.01	0.02	0.03	0.01	0.01	0.03	0.02	0.01	0.01
SiO	0.02	0.03	0.03	0.13	0.03	0.03	0.02	0.02	0.02
烧失量	42.35	36.76	41.36	42.59	41.39	37.01	39.25	43.82	41.05

其余氧化物含量均在 1% 以下。将 CaO 换算成 CaCO_3 后,9 件灰岩样品 CaCO_3 含量为 80.5% ~ 98.4%,其中 XYH-8 中 CaCO_3 含量最高达 98.4%。9 件灰岩样品中,除了 SiO_2 含量较高外,其余氧化物含量低于 1%。Al 和 Ti 含量常被用来反映陆源碎屑物质的混入程度,9 件灰岩样品的 Al_2O_3 和 TiO_2 含量分别为 0.03 ~ 0.76% 和 0.01 ~ 0.03%,其偏低的 Al_2O_3 和 TiO_2 含量表明灰岩成岩过程中陆源碎屑物质的影响较小。

陈多福等(2002)对冷泉碳酸盐岩的矿物组合特征进行研究,发现其矿物类型主要为镁方解石、白云石和文石,与传统的碳酸盐岩基本相同,但常以单一矿物为主。对洗鸭河灰岩显微组构进行观察,并结合主量元素分析结果,发现其矿物组成以细晶或泥晶碳酸盐矿物为主,含少量硅质碎屑和草莓状黄铁矿,表明洗鸭河灰岩矿物组成相对较为简单,与已有冷泉成因碳酸盐岩特征类似。

3.2 稀土元素

灰岩稀土元素分析结果列于表 2。经澳大利亚后太古宙平均沉积页岩(PAAS)(Taylor 和 McLennan, 1985)标准化后,灰岩稀土元素 PAAS 标准化配分形式图如图 3 所示。9 件灰岩 La/La^* 值介于 0.95 ~ 2.47, Pr/Pr^* 值介于 0.99 ~ 1.19, Ce/Ce^* 值介于 0.50 ~ 0.78, $\text{Dy}_{\text{PASS}}/\text{Sm}_{\text{PASS}}$ 值介于 1.12 ~ 2.30, $\text{La}_{\text{PASS}}/\text{Sm}_{\text{PASS}}$ 值介于 1.02 ~ 2.48。图 3 显示,灰岩稀土元素配分曲线形态平缓,REE 总量相对偏低,介于 2.62×10^{-6} ~ 43.49×10^{-6} , 平均 21.9×10^{-6} 。9 件灰岩均表现 Ce 负异常。已有研究指出,样品中 La 出现正异常时往往会对 Ce 异常值造成影响,因此,我们利用 $\text{Ce}/\text{Ce}^* - \text{Pr}/\text{Pr}^*$ 双变量图解(Bau et al. 1996)对灰岩的 Ce 异常值进行矫正,结果发现样品 XYH1、XYH8 和 XYH9 表现出的 Ce 负异常是因 La 正异常而造成的假,其余灰岩样品具有真实的 Ce 负异常(图 4)。

3.3 碳氧同位素

洗鸭河矿段中灰岩碳、氧同位素测试结果列于表 3。灰

岩碳同位素组成具有较大的变化范围,其 $\delta^{13}C_{V-PDB}$ 值介于 $-10.27\text{‰} \sim +3.736\text{‰}$ 之间,平均 -3.18‰ 。相比而言,样品 XYH10 更加富集较轻的碳同位素组成,XYH04 则相对浓集重的碳同位素组成。灰岩的 $\delta^{18}O_{V-PDB}$ 值表现基本一致,介于 $-8.20\text{‰} \sim -2.26\text{‰}$ 之间,平均 -6.04‰ 。

4 讨论

4.1 流体来源

通常情况下,冷泉环境下形成的碳酸盐岩明显亏损 ^{13}C 而具有极低的 $\delta^{13}C$ 值。然而,冷泉碳酸盐岩的碳源复杂多样,不同碳来源的冷泉碳酸盐岩具有截然不同的碳同位素组成,其 $\delta^{13}C$ 值相差较大。其中,与冷泉碳酸盐岩有关的烃类气体包括生物成因甲烷气和热解甲烷气。其中生物成因甲烷气体严重亏损 ^{13}C ,具有极低

表 2 贵州紫云洗鸭河泥盆系重晶石矿中灰岩稀土元素含量 ($\times 10^{-6}$) 及参数特征
Table 2 Rare earth element contents ($\times 10^{-6}$) and parameter characteristics of limestone in Devonian barite deposit in Xiyah, Ziyun County, Guizhou

编号	XYH1	XYH2	XYH3	XYH4	XYH5	XYH6	XYH7	XYH8	XYH9
La	3.13	5.89	11.50	7.90	2.89	11.80	6.09	0.87	2.98
Ce	3.19	9.13	13.00	6.97	3.29	13.80	7.94	0.93	3.90
Pr	0.39	1.32	1.95	1.30	0.53	2.09	1.23	0.10	0.42
Nd	1.66	4.72	7.94	5.56	2.16	8.13	4.46	0.32	1.52
Sm	0.23	0.81	1.41	0.96	0.41	1.45	0.85	0.05	0.35
Eu	0.06	0.20	0.26	0.36	0.09	0.35	0.16	/	0.06
Gd	0.33	0.99	1.48	1.18	0.30	1.58	0.82	0.10	0.46
Tb	0.05	0.15	0.25	0.21	0.08	0.28	0.14	0.01	0.09
Dy	0.22	0.97	1.56	1.29	0.49	1.59	0.83	0.10	0.48
Ho	0.06	0.21	0.34	0.31	0.10	0.34	0.21	0.01	0.13
Er	0.18	0.66	0.95	0.95	0.26	0.97	0.54	0.04	0.29
Tm	0.03	0.08	0.15	0.11	0.05	0.16	0.09	0.01	0.05
Yb	0.17	0.50	0.82	0.73	0.24	0.86	0.50	0.08	0.28
Lu	0.02	0.08	0.11	0.12	0.05	0.10	0.08	/	0.03
Σ REE	9.73	25.71	41.72	27.95	10.95	43.49	23.92	2.62	11.03
Ce/Ce*	0.63	0.76	0.63	0.50	0.61	0.64	0.67	0.69	0.78
Pr/Pr*	0.99	1.16	1.10	1.15	1.14	1.13	1.19	1.03	1.01
La/La*	2.47	0.95	1.65	1.96	1.49	1.41	1.08	1.67	1.50
Dy _{PASS} /Sm _{PASS}	1.12	1.42	1.31	1.59	1.41	1.30	1.16	2.30	1.65
La _{PASS} /Sm _{PASS}	1.99	1.06	1.19	1.19	1.02	1.18	1.05	2.48	1.25

注:稀土元素测试数据用澳大利亚后太古宙平均沉积页岩(PAAS)(Taylor 和 McLennan, 1985)进行标准化处理。“/”标示低于检测限。 $La/La^* = \frac{La_{PASS}}{3 \times Pr_{PASS} - 2 \times Nd_{PASS}}$, $Pr/Pr^* = \frac{2 \times Pr_{PASS}}{Ce_{PASS} + Nd_{PASS}}$, $Ce/Ce^* = \frac{2 \times Ce_{PASS}}{La_{PASS} + Pr_{PASS}}$ (Bau et al., 1996)。

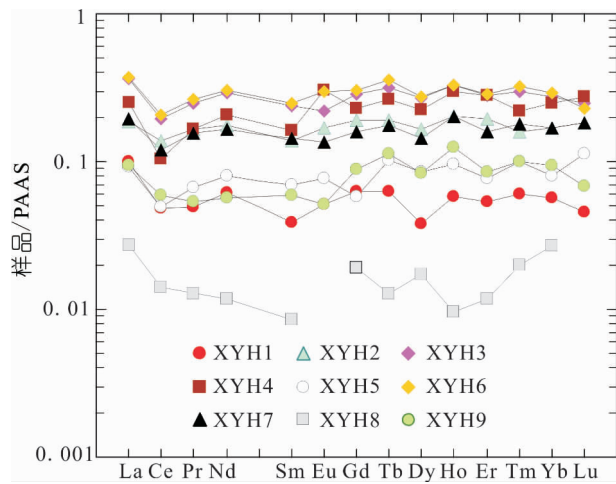


图 3 贵州紫云洗鸭河泥盆系重晶石矿中灰岩稀土元素 PASS 标准化配分模式图 (PASS 数据引自据 Taylor 和 McLennan, 1985)

Fig. 3 PAAS-normalized REE distribution patterns of limestone from Xiyah barite deposit in Ziyun, Guizhou (The data of PASS quoted from Taylor and McLennan, 1985)

的碳稳定同位素组成 ($\delta^{13}C_{V-PDB} = -40\text{‰} \sim -110\text{‰}$) (Whiticar, 1999); 热解成因甲烷气的碳同位素组成相比偏正,其 $\delta^{13}C_{V-PDB}$ 值介于 $-50\text{‰} \sim -30\text{‰}$ (Sackett, 1978)。另外一种原油等重烃类的化合物,其 $\delta^{13}C_{V-PDB}$ 值为 $-35\text{‰} \sim -25\text{‰}$ (Roberts et al., 1994)。研究发现,现代冷泉系统中自生碳酸盐岩的碳来源复杂,除了继承原始气体碳同位素组成特征外,还有正常海水溶解产生的碳和深部产甲烷作用残余 CO_2 中的碳混入,使得沉积碳酸盐岩的 $\delta^{13}C$ 值出现较大的变化范围 (Peckmann et al., 2004),从而更多地浓集重碳,这种现象在现代和古代冷泉碳酸盐岩中普遍发育 (Peckmann et al., 2004; 卞友艳等, 2012a; Tong Hongpeng et al., 2012; 欧莉华等, 2013; Canet et al., 2014; 夏国清等, 2015)。紫云洗鸭河灰岩 $\delta^{13}C_{V-PDB}$ 值为 $-10.27\text{‰} \sim +3.736\text{‰}$,介于热解成因气和石油烃类化合物碳同位素组成之间,暗示其碳源具有多来源的特征。这些研究工作指示,紫云洗鸭河灰岩的碳源,除了继承热解甲烷气化合物碳组成外,也承袭

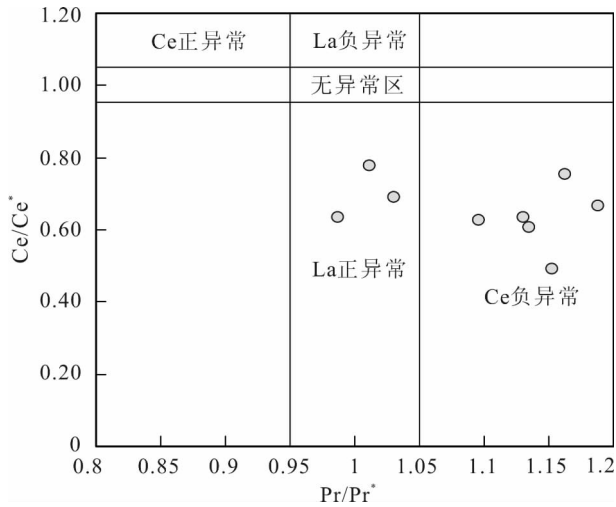


图4 贵州紫云洗鸭河重晶石矿床中灰岩 Ce 异常判别图(底图据 Bau et al., 1996)

Fig. 4 Ce/Ce* versus Pr/Pr* discrimination diagram for Ce anomaly of limestone from Xiyahé barite deposit in Ziyun, Guizhou (base map after Bau et al., 1996)

了正常海水或其他溶解无机碳。

已有研究表明,以石油等烃类化合物为主要碳源的冷泉沉积物中常残留有石油或沥青质痕迹 (Peckmann et al., 2001),这与紫云洗鸭河灰岩的岩石学和矿物学特征不符,说明灰岩中的碳不是来源于石油等烃类化合物。此外,碳源为有机质氧化成因的碳酸盐岩体在岩相学上会表现出样品颜色较深、在显微组构上会出现较多有机质残留的痕迹。洗鸭河灰岩结核多以浅灰色、灰色为主,在对灰岩进

表3 紫云洗鸭河重晶石矿床中泥盆系灰岩碳、氧同位素分析结果

Table 3 Carbon and oxygen isotopic compositions of the limestone from the Devonian barite deposit in Ziyun, Guizhou

采样位置	样号	$\delta^{13}\text{C}_{\text{V-PDB}} (\text{‰})$	$\delta^{18}\text{O}_{\text{V-PDB}} (\text{‰})$
洗鸭河	XYH1	1.097	-2.259
	XYH2	-1.995	-6.843
	XYH3	1.621	-5.498
	XYH4	3.736	-5.558
	XYH5	-7.569	-7.204
	XYH6	1.417	-6.10
	XYH7	-2.992	-6.30
	XYH8	-6.813	-6.773
	XYH9	-4.299	-3.617
	XYH10	-10.27	-8.10
	XYH14	-8.82	-8.20

行显微组构进行观察时也没有发现样品中出现有机质残留的痕迹,这些特征也表明洗鸭河灰岩的碳源不是有机质氧化的结果。高军波等(2015)研究了紫云泥盆系重晶石矿床赋矿硅质岩的 Si 同位素组成,认为其沉积过程中有热液硅的输入,说明重晶石和灰岩形成过程中有热液活动参与。另外,研究区及周边区域在晚泥盆纪时期广泛发育热水(液)成岩、成矿作用(高军波等, 2015),这些热事件将极大地加快烃类的成熟并转化为以热解成因甲烷气,说明紫云洗鸭河灰岩的碳源可能主要以热解成因甲烷气为主。

洗鸭河灰岩的 $\delta^{18}\text{O}_{\text{V-PDB}}$ 值为 $-8.20\text{‰} \sim -2.26\text{‰}$, 平均 -6.04‰ 。这与古代冷泉成因碳酸盐岩的氧同位素值类似 (Peckmann et al., 2001, 2004; Jiang Ganqing et al., 2003; Himmler et al., 2008; Wang Jiasheng et al., 2008), 与墨西哥湾西北部 Sonora 层状重晶石矿中冷泉成因碳酸盐岩 (Canet et al., 2014) 和我国西藏日喀则白垩世冷泉碳酸盐岩 (Tong Hongpeng et al., 2012) 的氧同位素值也比较接近, 但却低于现代海底冷泉碳酸盐岩的 $\delta^{18}\text{O}$ 值 (Canet et al., 2006; 冯东等, 2008; Roberts et al., 2010; Feng Dong et al., 2011)。研究表明: 由于成岩作用的影响, 中生代及更老时代的冷泉碳酸盐岩通常显示负的 $\delta^{18}\text{O}_{\text{V-PDB}}$ 值 (Campbell et al., 2002; Peckmann et al. 2001; Peckmann et al., 2004; Himmler et al., 2008; Hammer et al., 2011; Tong Hongpeng et al., 2012), 说明洗鸭河灰岩也普遍遭受了后期成岩作用的影响而使其 $\delta^{18}\text{O}_{\text{V-PDB}}$ 值偏向负值。利用氧同位素值示踪冷泉碳酸盐岩的物源区或流体来源, 除了要权衡后期成岩作用的影响外, 风化作用也会引起 $\delta^{18}\text{O}_{\text{V-PDB}}$ 值偏向负值 (Tong Hongpeng et al., 2012)。紫云洗鸭河矿段部分沉积硅质岩、灰岩遭受不同程度的氧化, 表面呈土黄色, 说明洗鸭河灰岩偏负的 $\delta^{18}\text{O}_{\text{V-PDB}}$ 值可能与氧化作用有关, 其对岩石成因、形成机理的指示意义不明显 (Tong Hongpeng et al., 2012)。

镇宁—紫云泥盆系重晶石矿床 $n(^{87}\text{Sr})/n(^{86}\text{Sr})$ 值介于 $0.70863 \sim 0.70898$, 平均 0.70877 (高军波等, 2013), 重晶石 $\delta^{34}\text{S}_{\text{V-CDT}}$ 值介于 $+27.6\text{‰} \sim +68.4\text{‰}$, 平均 $+52.2\text{‰}$ (Gao Junbo et al., 2016), 较同时期海水两者均表现明显的高值。而海底冷泉环境中形成的自生重晶石矿物或古代冷泉成因重晶石矿床普遍具有比沉积时海水偏高的锶同位素值和硫同位素组成 (Canet et al., 2014), 暗示镇宁—紫

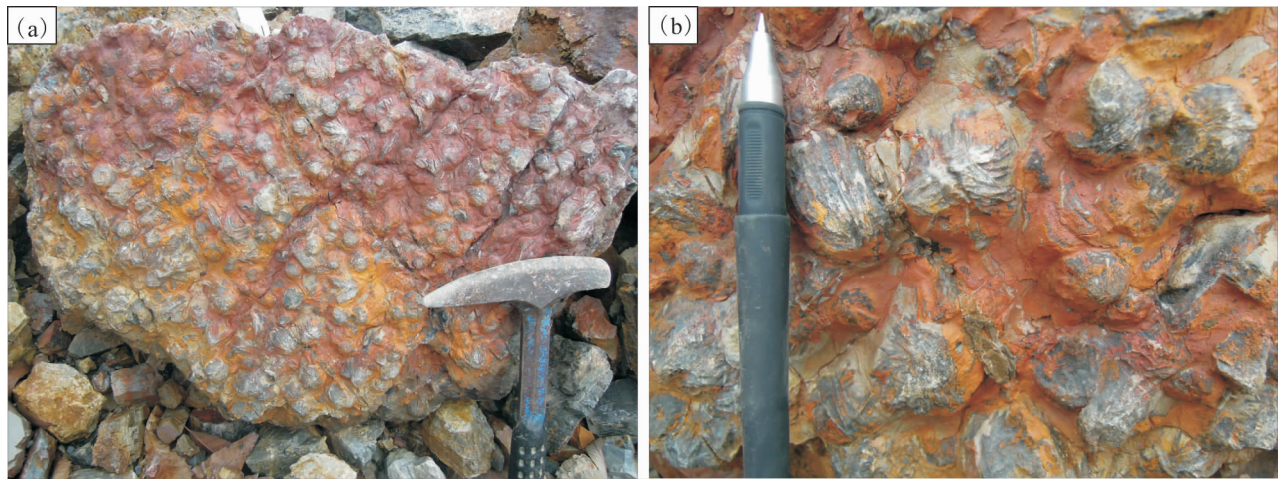


图5 贵州紫云洗鸭河重晶石矿中与甲烷渗漏有关的花瓣状重晶石

Fig. 5 Rosette barite associated with methane leakage from Xiyaher barite deposit in Ziyun, Guizhou

云泥盆系重晶石矿床成矿可能与古甲烷渗漏事件有关。此外,广泛分布在世界各地的新元古代“盖帽”碳酸盐岩已被大量的研究证明与古甲烷渗漏有关(Keddey et al., 2001, 2008; Jiang Ganqing et al., 2003; Wang Jiasheng et al., 2008),而这一时期与古甲烷渗漏事件有关的另一重要的标志性矿物为重晶石(Bao Huiming et al., 2008; Zhou Chuanming et al., 2010; Peng Yongbo et al., 2011),重晶石形貌特征多呈玫瑰花状、枝状、扇形等(王家生等, 2012),而类似结构类型重晶石在紫云泥盆系重晶石矿中也分布,其形貌特征呈花瓣状,组成花瓣的重晶石集合体大小基本一致(图 6a、b),说明紫云泥盆系重晶石成矿过程中可能存在古甲烷渗漏作用,这也从侧面进一步佐证了重晶石中的球状、椭球状和管状灰岩属于冷泉碳酸盐岩的认识。

4.2 形成环境

稀土元素 Ce 在无氧或缺氧环境中常以 Ce^{3+} 形式存在;当处于氧化环境时, Ce^{3+} 被氧化成 Ce^{4+} ,从而引起稀土元素分馏(王中刚等, 1989),因此,Ce 异常值常被用来示踪成岩、成矿过程的氧化还原状态。然而,后期成岩作用会对 Ce 异常值造成影响(Peckmann et al., 1999a; Shields et al., 2001)。当 $La_{PASS}/Sm_{PASS} > 0.35$,且 La_{PASS}/Sm_{PASS} 和 Ce/Ce^* 值之间无明显相关关系时,说明样品的稀土元素组成未受到后期成岩作用的影响(Mcarthur et al., 1984; Shields et al., 2001);当 Ce/Ce^* 值和 Dy_{PASS}/Sm_{PASS} 之间存在负相关关系时(图 6a 和 b),说明样品的稀土元素组成已受到后期成岩作用的影响(Shields et

al., 2001)。本文研究的 9 件灰岩样品 La_{PASS}/Sm_{PASS} 均大于 0.35,且 Ce/Ce^* 值与 La_{PASS}/Sm_{PASS} 和 Dy_{PASS}/Sm_{PASS} 之间均无明显相关性,说明它们所表现出的 Ce/Ce^* 值并未受到后期成岩作用的影响,反映了原始沉积物的特征及环境信息,可以用来进行成岩环境识别。

还原状态下的甲烷厌氧氧化作用是形成冷泉碳酸盐岩的最主要方式(Hinrichs et al., 1999),并以具有无 Ce 异常或 Ce 正异常为典型特征(Tong Hongpeng et al., 2012)。洗鸭河灰岩样品 XYH1、XYH8 和 XYH9 显示无真 Ce 异常,指示还原条件;其余灰岩样品均显示真 Ce 负异常(图 4),指示氧化条件,这些特征与墨西哥湾 BH 冷泉碳酸盐岩和摩洛哥 HM 中泥盆统冷泉碳酸盐岩类似(卞友艳等, 2012b),说明灰岩形成时的环境条件不是单一的还原状态,还存在间歇性的氧化作用。

已有研究发现,现代海底甲烷渗漏区的流体成分、成岩环境与甲烷流体的渗漏速率关系密切(Chen Duofu et al., 2005)。而海底冷泉流体的渗漏速率并非恒定不变,在不同时间段内常存在较大的差异(Tryon et al., 2004)。当冷泉流体以较低速率沿着运移通道排泄而形成的碳酸盐岩常具有较轻的 $\delta^{13}C$ 值,反之,其 $\delta^{13}C$ 值则明显偏重(Burton, 1993)。同时,渗漏速度较低的甲烷流体在大陆边缘沉积物中有利于形成氧化条件,特别是一些好氧氧化细菌和甲基氧化菌的反硝化作用可以产生氧,从而引起甲烷发生有氧氧化(Ettwing et al., 2010),形成地球化学指标显示氧化状态的冷泉碳酸盐岩

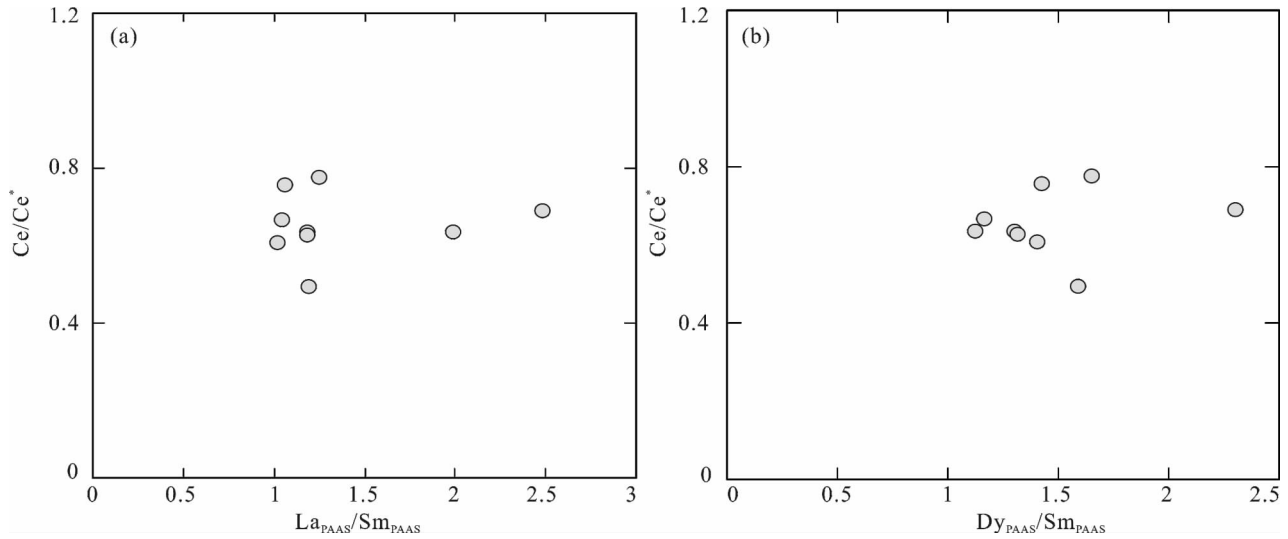


图6 成岩作用对贵州紫云洗鸭河重晶石矿中灰岩 Ce/Ce^* 值影响程度判别图解

Fig. 6 Iagram for discriminating the effect of diagenesis on Ce/Ce^* values of limestone from Xiyaher barite deposit in Ziyun, Guizhou

(冯东等, 2008; 卞友艳等, 2012)。诚然, 甲烷在有氧环境下氧化生成的 CO_2 对碳酸盐岩沉淀是极为不利的, 两者之间看似存在不可调节的矛盾。然而, 氧化环境下形成的冷泉碳酸盐岩的报道不断出现, 这已是不争的事实。通过对冷泉活动特征、流体性质及冷泉碳酸盐岩系统研究, 学者们(冯东等, 2008)认为, 氧化环境下发生碳酸盐岩沉淀, 渗漏流体需要具备两个方面的限制条件, 分别是渗漏速率低、渗漏速率间歇性, 说明形成洗鸭河灰岩的渗漏流体可能是以较低速率、间歇性排泄。

洗鸭河重晶石矿床中广泛分布大量球状、椭球状和管状灰岩, 灰岩中可见粒径介于 $30 \sim 100 \mu m$ 的碳酸盐岩凝块(图 2e)和草莓状黄铁矿(图 2g), 草莓状黄铁矿内部结构呈葵花状, 组成葵花状的单颗黄铁矿形态完整, 轮廓清晰(图 2h)。灰岩野外产状及其微观组构特征与现代和古代冷泉碳酸盐岩及从中观察到的黄铁矿结构极为类似(张美等, 2011; Tong Hongpeng et al., 2012; 欧莉华等, 2013; 夏国清等, 2015)。前人研究表明, 冷泉环境下的生物作用常可形成具有复杂内部结构的黄铁矿(Chen Duofu et al., 2006)。洗鸭河矿段中重晶石中已发现有棒状、哑铃状、球状细菌状化石(Gao Junbo et al., 2016), 说明灰岩成岩过程中可能有微生物作用参与。

5 结论

贵州紫云泥盆系重晶石矿床中分布大量球状、椭球状和管状灰岩, 灰岩顺层产于重晶石层之中或其下部。球状灰岩直径介于 $5 \sim 70 cm$, 管状灰岩长度介于 $10 \sim 60 cm$ 。灰岩中普遍发育类似现代海底冷泉碳酸盐岩的微—细晶碳酸盐岩凝块和草莓状黄铁矿, 草莓状黄铁矿内部结构呈葵花状, 组成葵花状的单颗黄铁矿大小基本一致, 轮廓清晰, 指示与生物作用有关。灰岩具有相对较轻的碳同位素组成, $\delta^{13}C_{V-PDB}$ 值最低为 -10.27% , 表明碳源主要为热解成因甲烷。灰岩 Ce/Ce^* 值除指示还原环境外, 也反映间歇性氧化作用的存在, 这可能与甲烷流体的渗漏速率有关。

致谢: 电镜扫描测试工作得到中国科学院地球化学研究所矿床地球化学国家重点实验室董少花老师的帮助! 陈多福教授为本文提出了建设性的意见, 使本文的研究内容得到进一步的提高, 论据更为充分; 成文过程得到审稿专家、责任编辑, 贵州大学资源与环境工程学院硕士研究生徐海、徐世林等细心矫正, 在此一并表示感谢!

参 考 文 献 / References

- 卞友艳, 陈多福. 2012a. 墨西哥湾北部上陆坡 Green Canyon 140 冷泉活动在自生碳酸盐岩中的地球化学记录. 地球化学, 42(3): 212 ~ 220.
- 卞友艳, 林治家, 冯东, 陈多福. 2012b. 冷泉碳酸盐岩的稀土元素

- 地球化学特征及氧化还原条件示踪. 热带海洋学报, 31(5): 37~44.
- 程裕淇. 1994. 中国区域地质概论. 北京: 地质出版社, 1~517.
- 陈多福, 陈先沛, 陈光谦. 2002. 冷泉流体沉积碳酸盐岩的地质地球化学特征. 沉积学报, 20(1): 34~40.
- 陈多福, 黄永祥, 冯东, 苏正, 陈光谦. 2005. 南海北部冷泉碳酸盐岩和石化微生物细菌及地质意义. 矿物岩石地球化学通报, 24(3): 185~189.
- 陈忠, 颜文, 陈木宏, 王淑红, 陆钧, 郑范, 向荣, 肖尚斌, 阎贫, 古森昌. 2006. 南海北部大陆坡冷泉碳酸盐结核的发现: 海底天然气渗漏活动的新证据. 科学通报, 51(9): 1065~1072.
- 杜远生, 黄虎, 杨海江, 黄宏伟, 陶平, 黄志强, 胡丽莎, 谢春霞. 2013. 晚古生代—中三叠世右江盆地的格局和转换. 地质论评, 59(1): 1~11.
- 冯东, 陈多福, 漆亮, Harry H. Roberts. 2008. 墨西哥湾 Alaminos Canyon 冷泉碳酸盐岩地质地球化学特征. 科学通报, 53(8): 966~974.
- 高军波, 杨瑞东. 2015. 水城—紫云—南丹深大断裂构造演化与泥盆纪热水(液)成岩、成矿效应. 贵阳: 贵州科技出版社, 1~224.
- 高军波, 杨瑞东, 陶平, 程伟, 刘坤, 何志威. 2013. 贵州镇宁泥盆系大型重晶石矿床镧同位素组成特征研究. 地球化学, 42(4): 285~392.
- 陆红锋, 陈芳, 刘坚, 廖志良, 孙晓明, 苏新. 2006. 南海北部神狐海区的自生碳酸盐岩烟囱——海底富烃流体活动的记录. 地质论评, 52(3): 352~357.
- 李艳菊, 史建南, 朱利东, 付修根, 杨文光, 杨若奔. 2013. 羌塘盆地双湖地区冷泉碳酸盐岩的发现及其天然气水合物成藏地质意义. 海洋地质与第四纪地质, 33(2): 105~110.
- 毛健全, 张启厚, 顾尚义. 1997. 水城阶断的地质特征及构造演化. 贵州工业大学学报, 26(2): 1~6.
- 欧莉华, 伊海生, 夏国清, 钱利军, 邱余波, 张超. 2013. 内蒙古东北部林西组碳酸盐岩结核的成因及油气地质意义. 成都理工大学学报(自然科学版), 40(4): 438~444.
- 王中刚, 于学元, 赵振华. 1989. 稀土元素地球化学. 北京: 科学出版社, 1~496.
- 王尚彦, 张慧, 王天华, 王纯厚, 彭成龙, 胡仁发, 陈明华, 石磊. 2006. 黔西水城—紫云地区晚古生代裂陷槽盆充填和演化. 地质通报, 25(3): 402~407.
- 王家生, 王舟, 胡军, 陈洪仁, 林杞. 2012. 华南新元古代“盖帽”碳酸盐岩中甲烷渗漏事件的综合识别特征. 地球科学(中国地质大学学报), 37(suppl 2): 14~22.
- 夏国清, 伊海生. 2015. 羌塘盆地双湖地区曲色组冷泉碳酸盐岩及其地质意义. 沉积与特提斯地质, 35(1): 68~75.
- 张美, 孙晓明, 芦阳, 徐莉, 陆红锋. 2011. 南海台西南盆地自生管状黄铁矿矿物学特征及其对天然气水合物的示踪意义. 矿床地质, 30(4): 725~734.
- 周琦, 杜远生, 颜佳新, 张命桥, 尹森林. 2007. 贵州松桃大塘坡地区南华纪早期冷泉碳酸盐岩地质地球化学特征. 地球科学, 32(6): 845~852.
- Bao Huiming, Lyons J R, Zhou Chuanming. 2008. Triple oxygen isotope evidence for elevated CO₂ levels after a Neoproterozoic glaciation. Nature, 453(7194): 504~506.
- Bau M, Koschinsky A, Dulski P, Hein J R. 1996. Comparison of the partitioning behaviours of yttrium, rare earth elements, and titanium between hydrogenetic marine ferromanganese crusts and seawater. Geochimica et Cosmochimica Acta, 60(10): 1709~1725.
- Bayon G, Birot D, Ruffine L, Caprais J C, Ponzevera E, Bollinger C, Donval J P, Charlou J L, Voisset M, Grimaud S. 2011. Evidence for intense REE scavenging at cold seeps from the Niger Delta margin. Earth and Planetary Science Letters, 312(3~4): 443~452.
- Bian Youyan, Chen Duofu. 2012a&. Cold seep activities recorded by geochemical characteristics of authigenic carbonates from Green Canyon 140, Gulf of Mexico. Geochemistry, 42(3): 212~220.
- Bian Youyan, Lin Zhijia, Feng Dong, Chen Duofu. 2012b&. Rare earth elements of seep carbonates and using them to trace redox variation at seep sites. Journal of Tropical Oceanography, 31(5): 37~44.
- Birgel D, Feng D, Roberts H H, Peckmann J. 2011. Changing redox conditions at cold seeps as revealed by authigenic carbonates from Alaminos Canyon, Northern Gulf of Mexico. Chemical Geology, 285(1~4): 82~96.
- Boetius A, Ravensschlag K, Schubert C J, Rickert D, Widdel F, Gleseke A, Amann R, Jergensen B B, Witte U, Pfannkuche O. 2000. A marine microbial consortium apparently mediating anaerobic oxidation of methane. Nature, 407(6804): 623~626.
- Burton E A. 1993. Controls on marine carbonate cement mineralogy: review and reassessment. Chemical Geology, 105(1~3): 163~179.
- Cheng Yuqi. 1994#. Brief introduction to regional geological tectonic of China. Beijing: Geological Publishing House, 1~517.
- Campbell K A, Farmer J D, Des Marais D. 2002. Ancient hydrocarbon seeps from the Mesozoic convergent margin of California: carbonate geochemistry fluids, and palaeoenvironments. Geofluids, 2(2): 63~94.
- Canet C, Anadón P, González-Partida E, Alfonso P, Rajabi A, Pérez-Segura E, Alba-Aldave L A. 2014. Paleozoic bedded barite deposits from Sonora (NW Mexico): evidence for a hydrocarbon seep environment of formation. Ore Geology Reviews, 56: 292~300.
- Canet C, Prol-Ledesma R M, Dando P R, Vázquez-Figueroa V, Shumilin E, Birosta E, Sánchez A J, Robinson C, Camprubí A, Tauler E. 2010. Discovery of massive seafloor gas seepage along the Wagner Fault, Northern Gulf of California. Sedimentary Geology, 228(3~4): 292~303.
- Canet C, Prol-Ledesma R M, Escobar-Briones E, Mortera-Gutiérrez C, Lozano-Santa Cruz R, Linares C, Cienfuegos E, Morales-Puente P. 2006. Mineralogical and geochemical characterization of hydrocarbon seep sediments from the Gulf of Mexico. Marine and Petroleum Geology, 23(5): 605~619.
- Chen Daizhao, Tucker M E, Jiang Maosheng, Zhu Jingquan. 2001. Long-distance correlation between tectonic-controlled, isolated carbonate platforms by cyclostratigraphy and sequence stratigraphy in the Devonian of South China. Sedimentology, 48(1): 57~78.
- Chen Duofu, Chen Xianpei, Chen Guangqian. 2002&. Geology and geochemistry of cold seepage and venting-related carbonates. Acta Sedimentologica Sinica, 20(1): 34~40.
- Chen Duofu, Feng Dong, Zheng Su, Zhi Guangsong, Chen Guangqian, Cathles L M. 2006. Pyrite crystallization in seep carbonates at gas vent and hydrate site. Materials Science and Engineering: C, 26(4): 602~605.
- Chen Duofu, Huang Yongxiang, Feng Dong, Su Zheng, Chen Guangqian. 2005&. Seep carbonate and preserved bacteria fossils in the Northern of the South China Sea and their geological implications. Bulletin of Mineralogy, Petrology and Geochemistry, 24(3): 185~189.
- Chen Duofu, Huang Yongxiang, Xun Laiyuan, Cathles L M. 2005. Seep carbonates and preserved methane oxidizing archaea and sulfate

- reducing bacteria fossils suggest recent gas venting on the seafloor in the Northeastern South China Sea. *Marine and Petroleum Geology*, 22(5): 613~621.
- Chen Zhong, Yan Wen, Chen Muhong Lu Jun, Zheng Fan, Xiang Rong, Xiao Shangbin, Yan ping, Gu Senchang. 2006#. Discovery of seep carbonate nodules in north of South China Sea; new evidence for the natural gas seep activity. *Chinese Science Bulletin*, 51(9): 1065~1072.
- Conti S, Fontana D, Mecozzi S, Panieri G, Pini G A. 2010. Late Miocene seep—carbonates and fluid migration on top of the Montepetra intrabasinal high (Northern Apennines, Italy): relations with synsedimentary folding. *Sedimentary Geology*, 231(1~2): 41~54.
- Du Yuansheng, Huang Hu, Yang Haijiang, Huang Hongwei, Tao Ping, Huang Zhiqiang, Hu Lisha, Xie Chunxia. 2013#. The basin translation from Late Paleozoic to Triassic of the Youjiang Basin and its tectonic signification. *Geological Review*, 59(1): 1~11.
- Ettwing K F, Butler M K, Paslier D L, Pelletier E, Mangelot S, Kuypers M M, Schreiber F, Dutilh B E, Zedelius J, de Beer D, Gloerich J, Wessels H J, van Alen T, Luesken F, Wu M L, van de Pas-Schoonen K T, Op den Camp H J, Janssen-Megens E M, Francoijs K J, Stunnenberg H, Weissenbach J, Jetten M S, Strous M. 2010. Nitrite-driven anaerobic methane oxidation by oxygenic bacteriar. *Nature*, 464(7288): 543~548.
- Feng Dong, Chen Duofu, Qi Liang, Roberts H H. 2008#. Seep carbonate geological and geochemical characteristics from Alaminos Canyon, Mexico bay. *Chinese Science Bulletin*, 53(8): 966~974.
- Feng Dong, Roberts H H. 2011. Geochemical characteristics of the barite deposits at cold seeps from the northern Gulf of Mexico continental slope. *Earth and Planetary Science Letters*, 309(1~2): 89~99.
- Gao, Junbo Yang Ruidong. 2015#. Tectonic evolution in Shuicheng—Ziyun—Nandan deep faults, Devonian hydrothermal fluid diagenesis and mineralization effect. Guiyang: Guizhou Science and Technology Press, 1~224.
- Gao Junbo, Yang Ruidong, Tao Ping, Chen Wei, Liu Kun, He Zhiwei. 2013#. Study of strontium isotope composition characteristics of large Devonian barite deposit from Zhenning, Guizhou. *Geochemica*, 42(4): 285~392.
- Gao Junbo, Yang Ruidong, Zheng Lulin, Cheng Wei, Chen Jun, Zhu Mingjin. 2016. Forming mechanism analysis of the abnormally high 834S baryte deposits: a case study from the Zhenning—Ziyun large Devonian baryte deposits, Guizhou Province, China. *Geomicrobiology Journal*, DOI: 10. 1080/01490451. 2015. 1137657.
- Ge Lu, Jiang Shaoyong. 2013. Sr isotopic compositions of cold seep carbonates from the South China Sea and the Panoche Hills (California, USA) and their significance in palaeoceanography. *Journal of Asian Earth Sciences*, 65(25): 34~41.
- Hammer Ø, Nakrem H A, Little C T S, Hryniewicz K, Sandy M R, Hurum J H, Druckenmiller P, Knutsen E M, Magne Høyberget M. 2011. Hydrocarbon seeps from close to the Jurassic—Cretaceous boundary, Svalbard. *Palaeogeography Palaeoclimatology Palaeoecology*, 306(1~2): 15~26.
- Hara H, Kurihar T, Kurod J, Adachi Y, Kurita H, Wakita K, Hisada K, Charusiri P, Charoentitrat T, Chaodumrong P. 2010. Geological and geochemical aspects of a Devonian siliceous succession in Northern Thailand; implications for the opening of the Paleo-Tethys. *Palaeogeography, Palaeoclimatology, Palaeoecology*, 297: 452~464.
- Himmeler T, Freiwald A, Stollhofen H, Peckmann J. 2008. Late Carboniferous hydrocarbon-seep carbonates from the glaciomarine Dwyka Group, Southern Namibia. *Palaeogeography, Palaeoclimatology, Palaeoecology*, 257(1~2): 185~197.
- Hinrichs K U, Hayes J M, Sylva S P, Brewer P G, DeLong E F. 1999. Methane-consuming archaeobacteria in marine sediments. *Nature*, 398(6730): 802~805.
- Hoffman P F, Kaufman A J, Halverson G P, Schrag D P. 1998. A Neoproterozoic snowball Earth. *Science*, 281(11): 1342~1346.
- Jenkins R G, Kaim A, Hikida Y, Tanabe K. 2007. Methane-flux-dependent lateral faunal changes in a Late Cretaceous chemosymbiotic assemblage from the Nakagawa area of Hokkaido, Japan. *Geobiology*, 5(2): 127~139.
- Jiang Ganqing, Kennedy M J, Christie-Blick N. 2003. Stable isotopic evidence for methane seeps in Neoproterozoic postglacial cap carbonates. *Nature*, 426(6968): 822~826.
- Kennedy M J, Christie-Blick N, Sohl L E. 2001. Are Proterozoic cap carbonates and isotopic excursions a record of gas hydrate destabilization following earth's coldest intervals? *Geology*, 29(5): 443~446.
- Kennedy M J, Mrofka D, Borch C. 2008. Snowball earth termination by destabilization of equatorial permafrost methane clathrate. *Nature*, 453(7195): 642~645.
- Lu Hongfeng, Chen Fang, Liu Jian, Liao Zhiliang, Sun Xiaoming, Su Xin. 2006#. Characteristics of authigenic carbonate chimneys in Shenhu area, Northern South China Sea; recorders of hydrocarbon-enriched fluid activity. *Geological Review*, 52(3): 352~357.
- Lu Yang, Sun Xiaoming, Lin Zhiyong, Lu Hongfeng. 2014. Authigenic carbonate mineralogy, South China Sea and its relationship with cold seep activity. *Acta Geologica Sinica*, 88(suppl 2): 1473~1474.
- Li Yanju, Shi Jiannan, Zhu Lidong, Fu Xiugen, Yang Wenguang, Yang Ruoyi. 2013#. The discovery of cold seep carbonate in the Shuanghu region, Qiangtang basin and its implication for gas hydrate accumulation. *Marine Geology & Quaternary geology*, 33(2): 105~110.
- Mao Jianquan, Zhang Qihou, Gu Shangyi. 1997#. Geological characteristics of Shuicheng fault and its tectonic evolution. *Journal of Guizhou University of technology*, 26(2): 1~6.
- Mearthur J M, Walsh J N. 1984. Rare-earth geochemistry of phosphorites. *Chemical Geology*, 47(3~4): 191~220.
- Ou Lihua, Yin Haisheng, Xia Guoqing, Qian Lijun, Qiu Yubo, Zhang Chao. 2013#. Origin and petroleum geological significance of carbonate rock concretes in Linxi Formation, Northeast of Mongolia, China. *Journal of Chengdu University of Technology (Science & Technology Edition)*, 40(4): 438~444.
- Peckmann J, Gischler E, Oschmann W, Reitner J. 2001. An Early Carboniferous seep community and hydrocarbon-derived carbonates from the Harz Mountains, Germany. *Geology*, 29(3): 271~274.
- Peckmann J, Thiel V. 2004. Carbon cycling at ancient methane-seeps. *Chemical Geology*, 205(3~4): 443~467.
- Peckmann J, Thiel V, Michaelis W, Clari P, Gaillard C, Martire L, Reitner J. 1999a. Cold seep deposits of beauvoisin (Oxfordian; Southeastern France) and marmorito (Miocene; Northern Italy): microbially induced authigenic carbonates. *International Journal of Earth Sciences*, 88(1): 60~75.
- Peckmann J, Walliser O H, Riegel W, Reitner J. 1999b. Signatures of hydrocarbon venting in a middle Devonian Carbonate Mound (Hollard Mound) at the Hamar Laghdad (Antiatlas, Morocco). *Facies*, 40(1): 281~296.

- Peng Yongbo, Bao Huiming, Zhou Chuanming, Yuan Xunlai. 2011. ^{17}O -depleted barite from two Marinoan cap dolostone sections, South China. *Earth and Planetary Science Letters*, 305(1~2): 21~31.
- Qi Liang, Hu Jing, Gregorie D C. 2000. Determination of trace elements in granites by inductively couple plasma mass spectrometry. *Talanta*, 51(3): 507~513.
- Roberts H H, Aharon P. 1994. Hydrocarbon-derived carbonate buildups of the Northern Gulf-of-Mexico continental-slope—a review of submersible investigations. *Geo-Marine Letters*, 14(2~3): 135~148.
- Roberts H H, Feng Dong, Joye S B. 2010. Cold-seep carbonates of the middle and lower continental slope, Northern Gulf of Mexico. *Deep Sea Research Part II*, 57(21~23): 2040~2054.
- Sackett W M. 1978. Carbon and hydrogen isotope effects during the thermocatalytic production of hydrocarbons in laboratory simulation experiments. *Geochimica et Cosmochimica Acta*, 42(6): 571~580.
- Shields G, Stille P. 2001. Diagenetic constraints on the use of cerium anomalies as palaeoseawater redox proxies: an isotopic and ree study of cambrian phosphorites. *Chemical Geology*, 175(1): 29~48.
- Stakes D S, Orange D, Paduan J B, Salmay K A, Maher N. 1999. Cold-seeps and authigenic carbonate formation in Monterey Bay. *Marine Geology*, 159: 93~109.
- Taylor S R, McLennan S M. 1985. *The Continental Crust: Its Composition and Evolution*. Blackwell, Oxford, 312.
- Tong Hongpeng, Chen Duofu. 2012. First discovery and characterizations of Late Cretaceous seep carbonates from Xigaze in Tibet. *Chinese Science Bulletin*, 57(33): 4363~4372.
- Tryon M D, Brown K M. 2004. Fluid and chemical cycling at Bush Hill: implications for gas- and hydrate-rich environments. *Geochemistry Geophysics Geosystems*, 5(12): 1~7.
- Wang Jiasheng, Jiang Ganqing, Xiao Shuhai, Li Qing, Wei Qing. 2008. Carbon isotope evidence for widespread methane seeps in the ~635Ma Doushantuo cap carbonate in south China. *Geology*, 36(5): 347~350.
- Wang Jiasheng, Wang Zhou, Hu jun, Chen Hongren, Lin Qi. 2012&. Multiple proxies indicating methane seepage during the Neoproterozoic cap carbonate in South China. *Earth Science—Journal of China University of Geosciences*, 37(suppl2): 14~22.
- Wang Zhonggang, Zhao Zhenhua. 1989#. *Rare earth elements geochemistry*. Beijing: Science Press, 1~496.
- Wang Shangyan, Zhang Hui, Wang Tianhua, Wang Chunhou, Peng Chenglong, Hu Renfa, Chen Minghua, Shi Lei. 2006&. Filling and evolution of the Late Palaeozoic Shuicheng—Ziyun aulacogen in Western Guizhou, China. *Geological Bulletin of China*, 25(3): 402~407.
- Wang Shuhong, Yan Wen, Chen Zhong, Zhang Nan, Chen Han. 2014. Rare earth elements in cold seep carbonates from the southwestern Dongsha area, Northern South China Sea. *Marine and Petroleum Geology*, 57: 482~493.
- Watanabe Y, Nakai S, Hiruta A, Matsumoto R, Yoshida K. 2008. U—Th dating of carbonate nodules from methane seeps off joetsu, Eastern margin of Japan sea. *Earth and Planetary Science Letters*, 272(1~2): 89~96.
- Whiticar M J. 1999. Carbon and hydrogen isotope systematics of bacterial formation and oxidation of methane. *Chemical Geology*, 161(1): 291~314.
- Wu Shiguo, Sakamoto I, Xu Jiren, Wong, H K. 2002. A comprehensive investigation of an offshore active fault in the Western Sagami Bay, Central Japan. *Acta Geologica Sinica (English Edition)*, 76(3): 300~307.
- Xia Guoqing, Yin Haisheng. 2015&. Characteristics and significance of the cold-vent carbonate rocks from the Quse Formation in the Shuanghu area, Qiangtang Basin, Northern Xizang. *Sedimentary Geology and Tethyan Geology*, 35(1): 68~75.
- Zhang Mei, Sun Xiaoming, Lu Yang, Xu Li, Lu Hongxiang. 2011&. Mineralogy of authigenic tube pyrite from the Southwest Taiwan Basin of South China Sea and its tracing significance for gas hydrates. *Mineral Deposits*, 30(4): 725~734.
- Zhou Chuanming, Bao Huiming, Peng Yongbo, Yuan Xunlai. 2010. Timing the deposition of ^{17}O -depleted barite at the aftermath of Nantuo glacial meltdown in South China. *Geology*, 38(10): 903~906.
- Zhou Qi, Du Yuansheng, Zhang Mingqiao, Yin Senlin. 2007&. Geological and geochemical characteristics of the cold seep carbonates in the Early Nanhua System in Datangpo, Songtao, Guizhou Province. *Earth Science—Journal of China University of Geosciences*, 32(6): 845~852.

Genesis of Devonian Spherical Limestone Related to Methane Seepage in the Xiyahé barite deposit, Ziyun, Southern Guizhou

ZHANG Xu¹⁾, GAO Junbo¹⁾, YANG Ruidong¹⁾, CHEN Jun¹⁾, ZHENG Lulin¹⁾, WEI Huairui¹⁾, BAO Miao²⁾

1) *College of Resources and Environmental Engineering, Guizhou University, 550025;*

2) *Bureau of Geology and Mineral Exploration and Development of Guizhou Province 112 Geological Brigade, Anshun, Guizhou, 561000*

Objectives: Although carbonates related to methane seepage seep were widely reported in modern sediment or sedimentary rocks (especially since Carboniferous), researches about cold seep carbonates associated with sedimentary deposits were rarely reported. In the study, we report the spherical, tubular limestone linked to the leakage of methane and other hydrocarbons, which was newly found in Xiyahé Devonian barite deposit, Guizhou Province.

Methods: A detailed field survey was conducted on Xiyahé Devonian barite deposits. 9 samples of limestone in the research were collected from Xiyahé section. In order to observe micro characteristics of the nodular

limestones, 9 limestone samples were observed by Polarization microscope in College of Resources and Environmental Engineering, Guizhou University and scan electron microscope in State Key Laboratory of Ore Deposit Geochemistry Chinese Academy Science, Guizhou, China.

The limestones were ground to less than 200 mesh for the use of X-Ray Diffraction (XRD), major element, stable carbon, oxygen isotope and rare earth element (REE) analyses. REE analyses were carried out in State Key Laboratory of Ore Deposit Geochemistry Chinese Academy Science, with ELAN DRC-e Q - ICP - MS made in Canada PerkinElmer. The major elements were measured with ME-XRF26d in ALS Minerals-ALS Chemex. Carbon and oxygen isotope analyses were carried out in the Key National Laboratory of Environmental Geochemistry of the Institute of Geochemistry under the Chinese Academy of Sciences. The instrument used was a gas-stable isotope mass spectrometer, which type is MAT253. The end results were corrected by carbonate rock solid standard. All analysis results were compared with the V-PDB standard. The precisions for $\delta^{13}\text{C}$ and $\delta^{18}\text{O}$ are better than $\pm 0.05\text{‰}$ and $\pm 0.08\text{‰}$ respectively.

Results: Carbonate clots and framboidal pyrites were found in the nodular limestones. The interior texture present sunflower shape in framboidal pyrites, single pyrite have clear outline and similar size. The $\delta^{13}\text{C}_{\text{V-PDB}}$ values of limestones in Xiyahe vary from -10.27‰ to $+3.736$, average value is -3.18‰ ; Xiyahe nodular limestone have relatively light oxygen isotope compositions with $\delta^{18}\text{O}_{\text{V-PDB}}$ values ranging from -8.20‰ to -2.26‰ , average value is -6.04‰ . The min-value of $\delta^{13}\text{C}_{\text{V-PDB}}$ of limestone is -10.27‰ . The total REE contents of 9 limestone samples in Xiyahe section range from 2.62×10^{-6} to 43.49×10^{-6} , average value is 21.9×10^{-6} . Ce/Ce^* values vary from 0.50×10^{-6} to 0.78×10^{-6} , but the revised results following Bau and Dulski's method (Bau et al. 1996) indicate real Ce anomaly occurrence in six samples, the others are not real Ce anomaly. Moreover, the major elements of limestone are mainly CaO and SiO_2 .

Conclusions: Amounts of nodular limestones were found in Xiyahe barite deposit. And the shape of limestones are spherical, elliptic spherical and tubular. The micro characteristics of nodular limestone are similar to modern cold seep carbonate (such as; carbonate clot, framboidal pyrite), and its carbon isotopes contents are also similar to modern carbonate associated with the leakage of methane. These results indicate the genesis of the nodular limestones in Xiyahe Devonian barite deposits was related to the leakage of methane and other hydrocarbons, but the petrographic observations of limestones and earlier studies on Xiyahe barite deposit suggest pyrolytic methane is the dominant carbon source of the limestone in Xiyahe barite deposit. The Ce anomaly of limestones show not only deoxidation in ancient sedimentary environment, but also intermittent oxidation are reflected. The situation may be affected by methane fluid leakage rate.

Keywords: Limestone; Sedimentary fabric; Carbon and oxygen isotope; Rare earth elements; Devonian; Ziyun.

Acknowledgements: We appreciated Professor Chen Duofu for constructive suggestions regarding revisions of the manuscript which significantly improved the manuscript, and thanks Zhang Yuxu for editorial handling. The project was funded by the National Natural Science Foundation of China (41503030), Guizhou Science and technology cooperation project (2015-7663), and the Talent Introduction Project of Guizhou University (201454).

First author: ZHANG Xu, male, born in 1991, Master Degree Candidate, engaged in the study of sedimentary deposits. Email: zhangxu199108@163.com.

Corresponding author: GAO Junbo, male, born in 1985, PHD, associate professor, engaged in teaching and research of sedimentary deposits. Email: gaojunbo1985@126.com

Manuscript received on: 2016-05-13; Accepted on: 2017-04-06; Edited by: ZHANG Yuxu.

Doi: 10.16509/j.georeview.2017.03.007